Bioorganic & Medicinal Chemistry 23 (2015) 6335–6345

Contents lists available at ScienceDirect

Bioorganic & Medicinal Chemistry

journal homepage: www.elsevier.com/locate/bmc

Revisiting 1,3,4-Oxadiazol-2-ones: Utilization in the Development of ABHD6 Inhibitors

Jayendra Z. Patel [a,*], John van Bruchem [a], Tuomo Laitinen [a], Agnieszka A. Kaczor [a,b], Dina Navia-Paldanius [c], Teija Parkkari [a], Juha R. Savinainen [c], Jarmo T. Laitinen [c], Tapio J. Nevalainen [a]

[a] School of Pharmacy, Faculty of Health Sciences, University of Eastern Finland, PO Box 1627, FIN-70211 Kuopio, Finland
[b] Department of Synthesis and Chemical Technology of Pharmaceutical Substances, Faculty of Pharmacy with Division of Medical Analytics, Medical University of Lublin, 4a Chodzki St., PL-20093 Lublin, Poland
[c] School of Medicine, Institute of Biomedicine/Physiology, University of Eastern Finland, PO Box 1627, FIN-70211 Kuopio, Finland

ARTICLE INFO

Article history:
Received 17 June 2015
Revised 6 August 2015
Accepted 25 August 2015
Available online 28 August 2015

Dedicated to Dr. Preeti Raval, principal scientist at Zydus Research Centre (ZRC, India).

Keywords:
α/β-Hydrolase domain-containing 6
2-Arachidonoylglycerol
Monoacylglycerol lipase
Fatty acid amide hydrolase
1,3,4-Oxadiazol-2-ones

ABSTRACT

This article describes our systematic approach to exploring the utility of the 1,3,4-oxadiazol-2-one scaffold in the development of ABHD6 inhibitors. Compound 3-(3-aminobenzyl)-5-methoxy-1,3,4-oxadiazol-2(3*H*)-one (JZP-169, **52**) was identified as a potent inhibitor of hABHD6, with an IC_{50} value of 216 nM. This compound at 10 μM concentration did not inhibit any other endocannabinoid hydrolases, such as FAAH, MAGL and ABHD12, or bind to the cannabinoid receptors (CB_1 and CB_2). Moreover, in competitive activity-based protein profiling (ABPP), compound **52** (JZP-169) at 10 μM selectively targeted ABHD6 of the serine hydrolases of mouse brain membrane proteome. Reversibility studies indicated that compound **52** inhibited hABHD6 in an irreversible manner. Finally, homology modelling and molecular docking studies were used to gain insights into the binding of compound **52** to the active site of hABHD6.

1. Introduction

The α/β-hydrolase domain-containing 6 (ABHD6) is an integral membrane serine hydrolase, accounting for ~4% of bulk 2-arachidonoylglycerol (2-AG) degradation in the central nervous system (CNS).[1] 2-AG is an endogenous cannabinoid ligand (endocannabinoid) which acts as a full agonist at the cannabinoid receptors CB1 and CB2.[2,3] In addition to ABHD6, there are two additional serine hydrolases in mouse brain tissue, monoacylglycerol lipase (MAGL) and α/β-hydrolase domain-containing 12 (ABHD12) which participate in 2-AG degradation, with the former enzyme accounting for the majority, 85%, and the latter for 9% of the hydrolytic activity, with the remainder of the degradation (~2%) being carried out by other enzymes, including fatty acid amide hydrolase (FAAH).[1,4] It is believed that ABHD6, MAGL and ABHD12 have different tissue distributions and subcellular localizations, giving rise to the possibility that all of these hydrolases have their own distinct roles in controlling the duration of action and fate of 2-AG.[1] It would be advantageous to develop selective ABHD6 inhibitors since these could help in dissecting the roles of these enzymes and obtaining an in-depth understanding of their physiological significance.

Several recent studies have identified ABHD6 as an emerging therapeutic target for the treatment of inflammation, metabolic disorders (obesity and type II diabetes mellitus) and epilepsy.[5–8] Moreover, it has been speculated that ABHD6 inhibitors may offer certain advantages over inhibitors of MAGL and ABHD12. Firstly, both a global genetic inactivation of MAGL and a chronic treatment with irreversibly acting MAGL inhibitors have evoked a substantial

Abbreviations: 2-AG, 2-arachidonoylglycerol; hABHD6, human recombinant α/β hydrolase domain 6; hMAGL, human recombinant monoacylglycerol lipase; hFAAH, human recombinant fatty acid amide hydrolase; hABHD12, human recombinant α/β hydrolase domain 12; WWL70, *N*-methyl-*N*-[[3-(4-pyridinyl)phenyl]-methyl]-4′-(aminocarbonyl)[1,1′-biphenyl]-4-yl carbamic acid ester; JZP-327A, *S*-3-(1-(4-isobutylphenyl)ethyl)-5-methoxy-1,3,4-oxadiazol-2(3*H*)-one; JZP-430, 4-morpholino-1,2,5-thiadiazol-3-yl cyclooctyl(methyl)carbamate; JZP-361, (4-(8-chloro-5*H*-benzo[5,6]cyclohepta[1,2-*b*]pyridin-11(6*H*)-ylidene)piperidin-1-yl)(1*H*-1,2,4-triazol-1-yl)methanone; THL, tetrahydrolipstatin (orlistat); PE, petroleum ether; EtOAc, ethyl acetate; DCM, dichloromethane.

* Corresponding author. Tel.: +358 40 355 3887.
E-mail addresses: jayendra.patel@uef.fi, jayorgchem137@gmail.com (J.Z. Patel).

http://dx.doi.org/10.1016/j.bmc.2015.08.030
0968-0896/

increase in brain 2-AG levels, triggering psychotropic side effects and cannabinoid receptor desensitization.[9–11] Secondly, genetically ABHD12 deficient mice display age-dependent symptoms that resemble a serious human neurodegenerative disorder, PHARC (polyneuropathy, hearing loss, ataxia, retinitis pigmentosa, and cataract).[12] In contrast, inhibition of ABHD6 causes only a marginal increase in brain 2-AG levels, evidence that ABHD6 inhibitors are likely to possess less CNS-related side-effects.[4,6,13]

At present, only a limited number of ABHD6 inhibitors have been described (Fig. 1). Cravatt's group prepared the first potent and selective carbamate-based ABHD6 inhibitor, WWL70 (**1**) using activity-based protein profiling (ABPP).[14] Marrs and colleagues synthesized UCM710 (**2**) and characterized it as a dual inhibitor of ABHD6 and FAAH.[15] Methylarachidonoyl fluorophosphonate (MAFP), orlistat (tetrahydrolipstatin, THL), RHC-80267, and the triterpene pristimerin have been identified as non-selective ABHD6 inhibitors.[16] Recently, Cravatt and coworkers noted that a carbamate-based compound, WWL123 (**3**), as well as triazole urea analogues such as KT195 (**4**) and KT182 (**5**), were potent and selective ABHD6 inhibitors.[17–19] Very recently, Janssen et al. revealed the glycine sulfonamide-based analogue LEI-106 (**6**) to be a highly selective dual inhibitor of sn-1-diacylglycerol lipase α (DAGL-α) and ABHD6.[20] In addition, we recently identified the 1,2,5-thiadiazole carbamate-based compound JZP-430 (**7**) as a potent and selective ABHD6 inhibitor and based on ABPP, it displayed good selectivity over other serine hydrolases in the mouse brain membrane proteome.[21]

Several research groups, including ours, have now described the exploitation of the 1,3,4-oxadiazol-2-one scaffold (Fig. 2, general structure **I** and **II**) in the development of serine hydrolases inhibitors.[22–30] For example, our chiral 1,3,4-oxadiazol-2-one (Fig. 2, general structure **II**) based compound *S*-3-(1-(4-isobutylphenyl)ethyl)-5-methoxy-1,3,4-oxadiazol-2(3*H*)-one (JZP-327A) was demonstrated to be a potent and reversible FAAH inhibitor.[29] In the same report, we also demonstrated that removal of the methyl group from the 3-position of 1,3,4-oxadiazol-2-ones led to the identification of 3-benzyl-1,3,4-oxadiazol-2-ones (Fig. 2, general structure **III**) which were dual FAAH–MAGL inhibitors. From the 1,3,4-oxadiazol-2-ones (**II** and **III**), we selected our previously reported compound **38** (see Table 1) for further optimization since it achieved ~40% inhibition of hABHD6 at a concentration of 1 μM but importantly no inhibition of hFAAH or hMAGL was evident at 10 μM.[29]

Here, building on our prior experience with the 1,3,4-oxadiazol-2-ones, we have now conducted a systematic structural modification of 3-benzyl-1,3,4-oxadiazol-2-ones and report activity data for these compounds against the endocannabinoid hydrolases (ABHD6, FAAH, MAGL and ABHD12). In addition, we evaluated their selectivity towards the cannabinoid receptors as well as

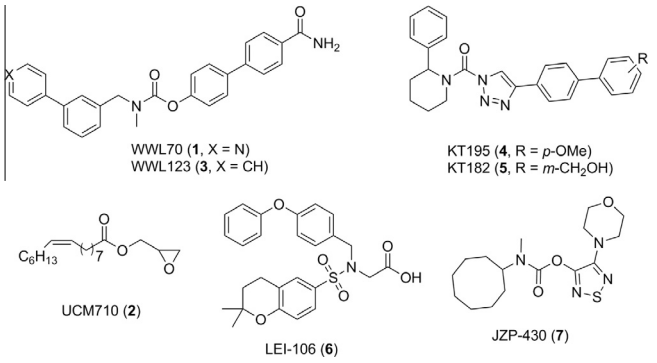

Figure 1. Representative structures of selective and non-selective ABHD6 inhibitors (**1**–**7**).

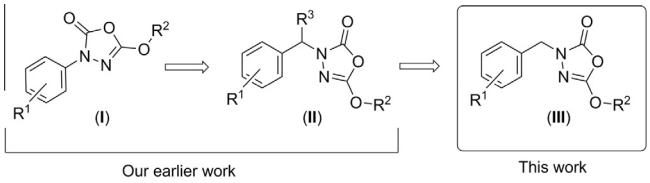

Figure 2. Advancement in 1,3,4-oxadiazol-2-ones (**I**–**III**).

towards mouse brain membrane serine hydrolases and the inhibitory data have been used to make a preliminary exploration of the structure–activity relationships (SARs). Finally, the reversibility of the synthesized compounds has been evaluated by both experimental approaches and molecular modelling.

2. Chemistry

The syntheses of 3-benzyl-1,3,4-oxadiazol-2-ones (**38**–**41**, **43**–**45** and **49**) have been reported in our earlier reports.[29,30] By utilizing the same procedure, several other analogues (**42**, **48**, **50**, **60**–**69** and **71**, Scheme 1) were also prepared by condensation of the appropriate aldehyde (**8**–**21**) with a suitable carbazate to produce a Schiff's base which was reduced to form the hydrazine carboxylate derivative (**22**, **25**–**37**) and subsequently cyclized with phosgene into 3-benzyl-1,3,4-oxadiazol-2-ones (**42**, **48**, **50**, **60**–**69** and **71**). Nitro containing 1,3,4-oxadiazol-2-ones (**48**–**50**, **69** and **71**) which had been obtained through Scheme 1 were reduced by 10% Pd/C to the corresponding amino derivatives (**51**–**53**, **70** and **72**, respectively, Scheme 1). Selected amino derivatives (**51**–**53**) were coupled with either acetyl or benzoyl chloride to produce the desired acetamides (**54**–**56**) and benzamides (**57**–**59**), respectively (Scheme 1). For the naphthalene analogues (**46** and **47**), the appropriate naphthaldehyde was used as the starting material as shown in Scheme 2. The synthesis of hydrazine carboxylate derivatives (**22**–**37**) was performed as according to published procedures with minor modifications (see Supporting information).

3. Results and discussion

3.1. Structure–activity relationships (SARs)

The inhibitory activities of the synthesized compounds were initially screened at a concentration of 1 μM against hABHD6 and hABHD12, and at 10 μM against hFAAH and hMAGL. The effects on hABHD6, hFAAH and hMAGL are presented in Tables 1 and 2, while those on hABHD12 appear in Table S2 (see Supplementary information).

As shown in Table 1, the unsubstituted analogue **38** displayed no inhibitory activity against either FAAH or MAGL. However, at a concentration of 1 μM, analogue **38** inhibited ABHD6 by ~40%. Analogues with bulky substituents on the *para* position of the benzyl moiety, such as isobutyl (compound **39**), Ph (compound **40**), and OPh (compound **43**), exhibited dual FAAH–MAGL inhibition. Switching the substituent from the *para* (compounds **40** and **43**) to the *meta* position (compounds **41** and **44**) resulted in a reduction in FAAH inhibitory activity. However, this change resulted in a complete loss of MAGL inhibition. Similarly, switching of the *para* substituents (compounds **40** and **43**) to the *ortho* position (compounds **42** and **45**) led to a marginal reduction, or even a complete loss of FAAH and/or MAGL inhibition. Among the analogues **38**–**45**, compounds **43**–**45** with a bulky OPh group only weakly (20–40%) inhibited ABHD6 at 1 μM concentration. From the bicyclic naphthalene analogues, the 1-naphthyl analogue **46** was inactive towards FAAH while the 2-naphthyl analogue **47** was a weak FAAH inhibitor (IC_{50} 3.98 μM). However, both analogues were inactive

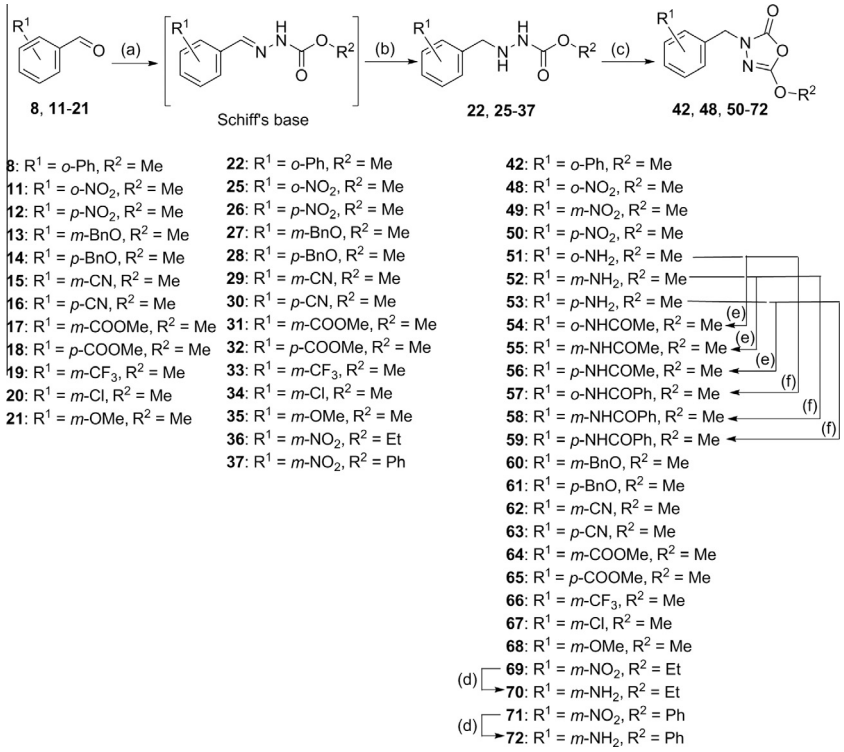

Scheme 1. Synthesis of 1,3,4-oxadiazol-2-ones **42**, **48**, **50**–**72**. Reagents and conditions: (a) $NH_2NHCOOR$,[2] MeOH, 4 Å molecular sieves, reflux, 2–16 h; (b) $NaBH_3CN$, MeOH, methanolic HCl, 0–25 °C, 24–72 h; (c) $COCl_2$, CH_2Cl_2, pyridine, 0–25 °C, 2–16 h (for compounds **60** and **61**, the reaction was carried out at −40 °C, 10 min); (d) 10% Pd/C, H_2 (atm), 20–25 °C, 4–8 h, MeOH; (e) MeCOCl, DCM, Et_3N, 0–25 °C, 16–24 h; (f) PhCOCl, DCM, Et_3N, 0–25 °C, 16–24 h.

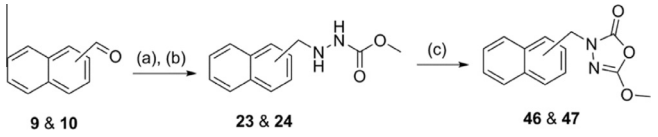

Scheme 2. Synthesis of 1,3,4-oxadiazol-2-ones **46** and **47**. Reagents and conditions: (a) $NH_2NHCOOMe$, MeOH, 4 Å molecular sieves, 3–4 drops AcOH, reflux, 2–16 h; (b) $NaBH_3CN$, MeOH, methanolic HCl, 0–25 °C, 24–72 h; (c) $COCl_2$, CH_2Cl_2, pyridine, 0–25 °C, 2–16 h.

towards MAGL while only the 1-naphthyl analogue weakly inhibited ABHD6 at 1 μM concentration. Since no significant improvements in ABHD6 inhibitory activity or selectivity over FAAH or MAGL were obtained with the bicyclic analogues **46** and **47**, we shifted our focus to study the electronic effect on unsubstituted analogue **38**.

With respect to the analogues with a smaller electron withdrawing group (EWG) nitro (compounds **48**–**50**), and for those analogues with an electron releasing group (ERG) amino (compounds **51**–**53**), it was found that substituents at different positions on the benzyl moiety present at the 3-position of 1,3,4-oxadiazol-2-ones were inactive towards FAAH and MAGL. However, *ortho*- and *meta*-NO_2 substituted analogues (compounds **48** and **49**) showed weak ABHD6 inhibition at a concentration of 1 μM while the *meta*-amino analogue **52** showed significant ABHD6 inhibition with an IC_{50} value of 216 nM. Protection of the amino group in compounds **51**–**53** with an acetyl group (compounds **54**–**56**) achieved no improvement of FAAH and MAGL inhibition. The loss of ABHD6 inhibition seen with the *meta*-substituted compound **55** revealed the importance of the free amino group of compound **52**. In contrast, protection with the bulky benzoyl group of compounds **51**–**53** (compounds **57**–**59**) resulted in enhanced FAAH and MAGL inhibition for the *para*-substituted analogue **59** over its *meta* (compound **58**) and *ortho* (compound **57**) counterparts, in line with previous findings with the bulky *para*-substituted compounds **40** and **43**. As expected, analogues **60** and **61**, possessing bulky benzyloxy substituents at their *meta* and *para* positions respectively, displayed improved abilities to inhibit both FAAH and MAGL. Moreover, the *meta*-benzyloxy analogue (compound **60**) inhibited ABHD6 by nearly 50% at a concentration of 1 μM. The majority of the analogues having either smaller EWGs at either *meta* (compounds **62**, **64**, **66** and **67**) or *para* positions (compounds **63** and **65**) or smaller ERG at the *meta* position (compound **68**) were found to be inactive towards FAAH and MAGL although analogue **65** which had a *para* substituted EWG did exhibit weak FAAH inhibition. Moreover, among these analogues, only *meta*-substituted analogues **62**, **67** and **68** appreciably inhibited ABHD6 whereas compounds **64** and **66** inhibited ABHD6 in the sub-micromolar range with IC_{50} values of 0.45 and 0.87 μM, respectively.

As shown in Table 2, replacement of the methoxy group present at the 5-position of 1,3,4-oxadiazol-2-ones in compounds **49** and **52** with an ethoxy group (compounds **69** and **70**) resulted in the loss of inhibitory activities towards all studied enzymes, with the sole exception being compound **69** which at 1 μM concentration weakly inhibited ABHD6. However, when a phenoxy group was incorporated (compounds **71** and **72**), the compounds inhibited FAAH weakly and MAGL moderately whereas they potently inhibited ABHD6 (IC_{50} values of 0.13 and 0.073 μM, respectively). Overall, analogues with a bulky or smaller *meta* substituent displayed weak to considerable ABHD6 inhibition; among these, amino analogues **52** and **72** in particular showed much improved ABHD6 inhibition (see Tables 1 and 2). Finally, we further tested compound **52** at a higher concentration (20 μM) to obtain an indication of selectivity towards putative significant off-targets, FAAH and MAGL. Compound **52** still

Table 1
Inhibitory activities of 1,3,4-oxadiazol-2-ones **38–68**[*] towards FAAH, MAGL and ABHD6

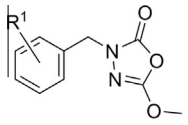

38-45, 48-68

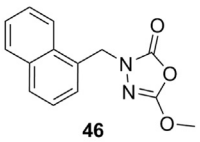

46

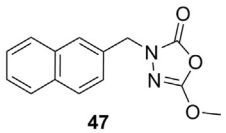

47

Compd	R^1	pIC_{50} ± SEM [IC_{50}, μM][a]		
		% inhibition at 10 μM[b]		% remaining enzymatic ABHD6 activity at 1 μM[c]
		hFAAH	hMAGL	hABHD6
38	H	NI [d]	NI	61%
39	*p*-Isobutyl	7.05 ± 0.09 [0.091]	5.87 ± 0.13 [1.3]	NI
40	*p*-Ph	6.79 ± 0.10 [0.16]	5.79 ± 0.15 [1.6]	NI
41	*m*-Ph	46%	32%	NI
42	*o*-Ph	23%	8%	NI
43	*p*-OPh	7.0 ± 0.06 [0.10]	6.40 ± 0.23 [0.40]	77%
44	*m*-OPh	6.01 ± 0.05 [0.98]	15%	70%
45	*o*-OPh	5.20 ± 0.13 [6.3]	NI	60%
46	—	35%	11%	64%
47	—	5.40 ± 0.21 [3.98]	NI	NI
48	*o*-NO_2	36%	43%	57%
49	*m*-NO_2	7%	32%	65%
50	*p*-NO_2	18%	36%	NI
51	*o*-NH_2	8%	4%	NI
52 (JZP-169)	*m*-NH_2	18% (41% at 20 μM)	21% (33% at 20 μM)	6.66 ± 0.04 [0.216] [e]
53	*p*-NH_2	34%	23%	NI
54	*o*-NHCOMe	11%	3%	NI
55	*m*- NHCOMe	NI	12%	NI
56	*p*-NHCOMe	37%	16%	NI
57	*o*-NHCOPh	NI	NI	NI
58	*m*-NHCOPh	NI	48%	79%
59	*p*-NHCOPh	6.21 ± 0.12 [0.62]	6.25 ± 0.08 [0.56]	88%
60	*m*-OBn	5.82 ± 0.06 [1.51]	5.49 ± 0.04 [3.23]	53%
61	*p*-OBn	6.39 ± 0.08 [0.41]	6.28 ± 0.07 [0.52]	NI
62	*m*-CN	NI	23%	63%
63	*p*-CN	NI	25%	NI
64	*m*-COOMe	20%	7%	6.35 ± 0.05 [0.45]
65	*p*-COOMe	5.17 ± 0.06 [6.76]	15%	NI
66	*m*-CF_3	12%	48%	6.06 ± 0.05 [0.87]
67	*m*-Cl	37%	43%	52%
68	*m*-OMe	NI	6%	70%
JZP-327A[e]	—	7.94 ± 0.05 [0.011]	16%	NI
JZP-430 (**7**)[f]	—	18%	NI	7.36 ± 0.05 [0.044]
JZP-361[g]	—	5.14 ± 0.08 [7.24]	7.34 ± 0.12 [0.046]	5.75 ± 0.04 [1.78]

[*] Compounds **38–41**,[29] **43–45**[29] and **49**[30] had been reported earlier but are included here to provide better insights into SARs.
[a] pIC_{50} values ($-\log_{10}$ [IC_{50}]) represent the mean ± SEM from three independent experiments performed in duplicates for the most potent compounds while for the less active ones, values from two independent experiments were used.
[b] The percentage (%) of inhibition is represented as the mean from two independent experiments performed in duplicate.
[c] Remaining activity (%) at 1 μM is given when it is <90%.
[d] NI, no inhibition.
[e] *S*-3-(1-(4-Isobutylphenyl)ethyl)-5-methoxy-1,3,4-oxadiazol-2(3*H*)-one (JZP-327A)[29] was used as a reference FAAH inhibitor.
[f] 4-Morpholino-1,2,5-thiadiazol-3-yl cyclooctyl(methyl)carbamate (JZP-430)[21] was used as a reference ABHD6 inhibitor.
[g] (4-(8-Chloro-5*H*-benzo[5,6]cyclohepta[1,2-*b*]pyridin-11(6*H*)-ylidene)piperidin-1-yl)(1*H*-1,2,4-triazol-1-yl)methanone (JZP-361)[31] was used as a reference MAGL inhibitor.

Table 2
Inhibitory activities of 1,3,4-oxadiazol-2-ones **69–72** towards FAAH, MAGL and ABHD6

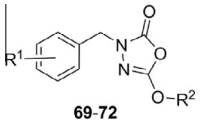

69-72

Compd	R^1	R^2	pIC_{50} ± SEM [IC_{50}, μM][a]		
			% inhibition at 10 μM[b]		% remaining enzymatic ABHD6 activity at 1 μM[c]
			hFAAH	hMAGL	hABHD6
69	*m*-NO_2	Et	NI[d]	30%	63%
70	*m*-NH_2	Et	10%	15%	NI
71	*m*-NO_2	Ph	38%	5.49 ± 0.06 [3.31]	6.88 ± 0.05 [0.13]
72 (JZP-JVB-053)	*m*-NH_2	Ph	25%	5.1 ± 0.08 [7.94]	7.13 ± 0.05 [0.073]

[a–d] See footnotes for Table 1.

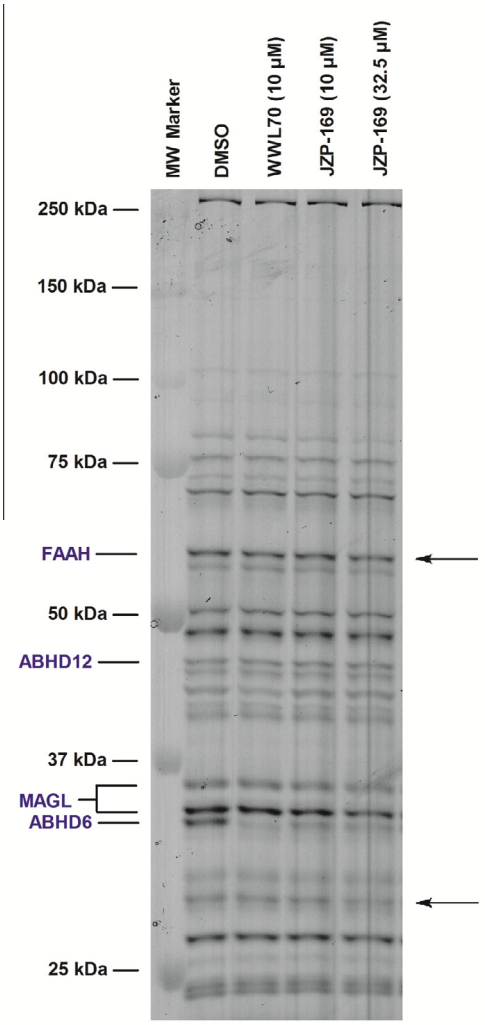

Figure 3. Competitive ABPP reveals the selectivity of compound **52** (JZP-169) among the serine hydrolases of mouse whole brain membrane proteome. Molecular weight markers are indicated on the left. The reference inhibitor WWL70 (**1**) was used at the indicated concentration to indicate the ABHD6 protein band.[14] At a concentration of 10 μM, compound **52** (JZP-169) selectively targeted ABHD6 as probe labelling to other visible serine hydrolases was not affected. However, at very high concentration (32.5 μM) FAAH and additional serine hydrolase (indicated by black arrows) appear as off-target of this compound. The gel is representative from two ABPP experiments with similar outcomes.

caused less than 50% inhibition towards both of these enzymes (see Table 1) thereby achieving nearly >90-fold selectivity towards ABHD6 over FAAH and MAGL.

Table 4
Inhibition of ABHD6 by JZP-169 (**52**) and JZP-430 (**7**) indicates the irreversible mode of inhibition after a rapid 40-fold dilution of inhibitor-treated hABHD6 preparation

Incubation time (min)	pIC_{50} ± SEM		
	JZP-169 (**52**)	JZP-430 (**7**)	THL
10	5.39 ± 0.08	7.04 ± 0.03	7.88 ± 0.05***
30	5.42 ± 0.07	7.06 ± 0.03	7.85 ± 0.04***
60	5.44 ± 0.06	7.06 ± 0.03	7.70 ± 0.06**
90	5.48 ± 0.05	7.03 ± 0.03	7.43 ± 0.06

In contrast to compounds (**52**) and (**7**), potency of THL significantly declines during the 90 min incubation (an asterisk denotes a statistically significant difference compared to the pIC_{50} value at 90 min time-point: one-way Anova, followed by Tukey's multiple comparison test (p <0.01**, p <0.001***)). Data are means ± SEM from three to seven independent experiments. Note also that due to methodological limitations, the IC_{50} values obtained by the dilution method are not directly comparable to those obtained using the routine assay protocol.[34,38]

3.2. Selectivity among serine hydrolases and cannabinoid receptors

(I) Activity based protein profiling (ABPP).

Next, we explored in more detail the selectivity of the 1,3,4-oxadiazol-2-one analogues JZP-169 (**52**) and JZP-JVB-053 (**72**) using competitive ABPP of the mouse brain membrane proteome. We used earlier reported inhibitor WWL70[14] (**1**) at the indicated concentration to locate the band of ABHD6. As shown in Figure 3, JZP-169 (**52**) at 10 μM concentration efficiently competed with probe binding to ABHD6 but no visible effect on other serine hydrolases could be detected by this approach. Only at a very high concentration of 32.5 μM did JZP-169 (**52**) inhibit the other serine hydrolases (indicated by black arrows). JZP-JVB-053 (**72**) achieved almost complete inhibition of the ABHD6 band at 1 μM (Fig. S1, see Supporting information) although at a 10-fold concentration it targeted also other serine hydrolases. In brief, when tested at 10 μM, JZP-169 (**52**) appeared to be selective for ABHD6 over the other recognized brain serine hydrolases, including FAAH, MAGL and ABHD12.

(II) Selectivity over the cannabinoid receptors.

To rule out cross-activity with additional targets of the endocannabinoid system, compound JZP-169 (**52**), which appeared to be the best ABHD6 inhibitor in this series in terms of potency and selectivity, was evaluated for its possible agonist or antagonist activity at the cannabinoid CB_1 and CB_2 receptors, using a previously validated [^{35}S]GTPγS binding assay.[32,33] In this system, compound **52** did not display any significant agonist or antagonist activities when tested at 10 μM concentration (Table 3).

Table 3
Activity of compound JZP-169 (**52**) at CB1 and CB2 receptors

Compd	Agonist activity		CB_1R antagonist activity[a]
	CB_1R[a] [^{35}S]GTPγS binding % basal (mean (range), n = 2)	CB_2R[b]	[^{35}S]GTPγS binding % HU210-evoked response (mean (range), n = 2)
JZP-169 (**52**)	96 (92–100)	107 (102–111)	104 (101–106)
HU210 (1 μM)	306 (302–311)	–	–
HU210 (10 nM)	–	167 (165–169)	–
AM251 (1 μM)	–	–	38 (36–40)
SR144528 (1 μM)	–	56 (54–59)	–

[a] Rat cerebellar membranes.
[b] hCB_2R-CHO cell membranes.

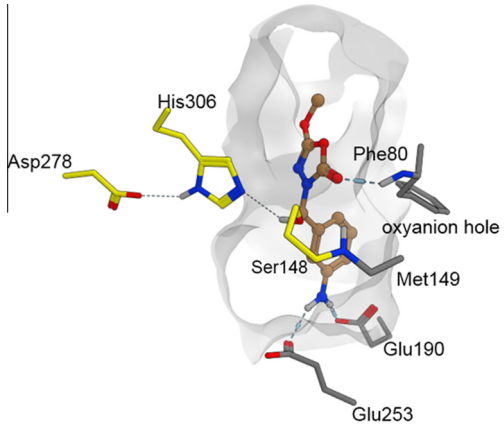

Figure 4. Most favourable Glide docking pose of compound **52** (JZP-169) into the ABHD6 active site in a homology model. Catalytic residues are coloured using yellow carbons and the surface of the active site is presented.

3.3. Reversibility of ABHD6 inhibition

To explore in more detail the ABHD6-binding mode of JZP-169 (**52**), we tested its ability to inhibit hABHD6 using a 96-well format dilution method suitable for testing compound reversibility.[34] In this assay, our previously reported irreversible ABHD6 inhibitor JZP-430 (**7**)[21] and compound JZP-169 (**52**) fully retained their potencies during the 90 min incubation period after a rapid 40-fold dilution of the enzyme–inhibitor complex (Table 4) suggesting that in these time-frame studies, JZP-169 inactivated hABHD6 in an irreversible manner. In contrast, the inhibitory properties of orlistat (tetrahydrolipstatin, THL) were significantly reduced during the 90 min incubation, indicating that this compound functioned as a reversible ABHD6 inhibitor. The inactivation of ABHD6 by 1,3,4-oxadiazol-2-one based compound JZP-169, and THL are quite remarkable. This is because our previously reported 1,3,4-oxadiazol-2-one based compound JZP-327A inhibited FAAH in a reversible manner[29] whereas here the 1,3,4-oxadiazol-2-one based compound JZP-169 inhibited ABHD6 irreversibly. It is also noteworthy that THL is generally believed to irreversibly inhibit serine hydrolases such as pancreatic lipase[35,36] and ABHD12[37] while the present studies show that it inhibited ABHD6 in a reversible manner.

3.4. Molecular modelling

Subsequently, we conducted a molecular docking study of our compound **52** (JZP-169) (see Fig. 4) with a previously generated homology model.[21] The catalytic machinery of several serine hydrolases consists of a catalytic triad supplemented by an oxyanion hole to allow the activation of the carbonyl carbon. Previous docking studies have indicated that inhibitory activity can be partly explained by means of easy access to the residues making up the oxyanion hole along with good shape complementarity between the enzyme and ligand. JZP-169 achieved good docking convergence by making hydrogen bond interactions with the oxyanion hole (main chain amide of Phe80) when the putative nucleophile Ser148 was in close vicinity to the carbonyl carbon ready for nucleophilic attack. Furthermore, our homology model and docking studies suggested that the amino group present at the *meta*-position in this 3-benzyl-1,3,4-oxadiazol-2-one was able to make hydrogen bond contact with the side chains of Glu190 and Glu253, which may have enhanced its inhibitory activity by stabilizing the covalent reaction intermediate or slowing the rate of the product release.

Molecular modelling was used to confirm the irreversibility of JZP-169 (**52**) along with other established irreversible ABHD6 inhibitors (WWL70 (**1**), KT182 (**5**) and JZP-430 (**7**)) and a reversible inhibitor, THL. First, HOMO and LUMO energy and the HOMO–LUMO gap for the studied inhibitors were calculated with Gaussian09 (Table 5). It was found that the irreversible inhibitors, JZP-169, JZP-430, KT182 and WWL70 could be characterized with a lower HOMO–LUMO gap than could be obtained with THL, that is, they were more reactive. In order to investigate in detail the reversibility of the investigated inhibitors, the QM/MM approach of Discovery Studio 3.1 was applied; this is a well-established technique for this purpose.[39] This method was used to minimize hypothetical covalent complexes and respective transition state complexes on the QM/MM level and to calculate their final energy. For the transition state systems, it was assumed that the carbonyl group of the ligands reacted with the side chain of Ser^{148} as earlier reported.[19,40] The data are presented in Table 5. It can be seen that THL (orlistat) displayed an energy of activation of complex dissociation below 20 kcal/mol, which is the energy barrier for reactions at room temperature.[41] In contrast, the activation energies for dissociation of JZP-169, JZP-430, KT182 and WWL70 were over 20 kcal/mol, meaning that these inhibitors would be irreversible at room temperature. This may be caused by carbamoylation of Ser^{148} by the irreversible inhibitors which leads to trapping of this residue within an acyl-enzyme like intermediate (carbamoyl serine structure) as earlier reported.[19,40]

Table 5
Selected parameters for the compounds involved in reversibility studies

Compd	HOMO (kcal/mol)	LUMO (kcal/mol)	HOMO–LUMO gap (kcal/mol)	Energy of activation of complex dissociation (kcal/mol)
JZP-169 (**52**)	−8.408	0.180	8.587	36.181
JZP-430 (**7**)	−8.758	−0.533	8.224	42.530
KT182 (**5**)	−8.810	−0.371	8.438	37.454
WWL70 (**1**)	−9.133	−0.491	8.642	34.226
THL	−10.143	0.658	10.801	17.541

4. Conclusions

To summarize, a convenient synthesis of 3-benzyl-1,3,4-oxadiazol-2-ones was developed and out of the series of compounds synthesized, JZP-169 (**52**) was identified as a potent hABHD6 inhibitor (IC_{50} = 214 nM), having >90-fold selectivity over other principal off-targets such as FAAH and MAGL. Competitive ABPP indicated that compound **52** selectively targeted ABHD6 in preference over other serine hydrolases in the mouse brain membrane proteome. Moreover, the detailed inhibition mechanism studies conducted with both experimental assays and molecular modelling indicated that compound **52** acted as an irreversible inhibitor of hABHD6. Molecular modelling studies further demonstrated that compound **52** underwent favourable interactions within the active site of hABHD6, including important hydrogen-bonding of the carbonyl oxygen to the oxyanion hole. Moreover, within the still restricted classes of known ABHD6 inhibitors, the 1,3,4-oxadiazol-2-one scaffold represents a novel class of compounds. Finally, 1,3,4-oxadiazol-2-one represents a versatile scaffold for the further development of inhibitors with diverse mechanisms targeting other serine hydrolases.

5. Experimental

5.1. Materials and methods

All reagents and solvents were purchased from commercial suppliers and were used without further purification. Reactions

were monitored by thin-layer chromatography (TLC) using aluminium sheets coated with silica gel F_{245} (60 Å, 40–63 μm, 230–400 mesh) with suitable UV visualization. Purification was carried out by flash chromatography (FC) on J.T. Baker's silica gel for chromatography (pore size 60 Å, particle size 50 nm) or by RediSep® normal-phase silica flash columns using CombiFlash Companion (Teledyne Isco, USA). Petroleum ether (PE) of fraction 40–60 °C was used for chromatography. ^{1}H NMR and ^{13}C NMR were recorded on a Bruker Avance AV 500 (Bruker Biospin, Switzerland) spectrometer operating on 500.1 and 125.8 MHz, respectively. Tetramethylsilane (TMS) was used as an internal standard for ^{1}H NMR. Chemical shifts are reported in ppm on the δ scale from an internal standard of solvent ($CDCl_3$ 7.26 and 77.0 ppm, DMSO 2.50). All spectra were processed from the recorded FID files with TOPSPIN 2.1 software or ACD/NMR Processor Academic Edition. The following abbreviations are used: s, singlet; br s, broad singlet; d, doublet; t, triplet; q, quartet; m, multiplet. The coupling constants are reported in Hz. ESI-MS spectra were acquired using an LCQ quadrupole ion trap mass spectrometer equipped with an electrospray ionization source (Thermo LTQ, San Jose, CA, USA). Elemental analyses were performed on a ThermoQuest CE instrument (EA 1110 CHNS-O) or a Perkin–Elmer PE 2400 Series II CHNS-O Analyzer. The purity of the synthesized 1,3,4-oxadiazol-2-ones (**42**, **46**–**48**, **50**–**72**) are ⩾95% (see Table S1 of Supplementary information).

5.1.1. General procedures for preparation of novel 1,3,4-oxadiazol-2(3*H*)-ones (42, 46–48, 50, 60–69 and 71)

The 1,3,4-oxadiazol-2-one (**42**, **46**–**48**, **50**, **60**–**69** and **71**) were prepared according to our earlier reported method with minor modifications.[29] To a solution of appropriate hydrazine carboxylate (**22**–**37**) (1.0 equiv) in dichloromethane (0.2 M) pyridine (3.0 equiv) was added at 0 °C followed by a drop wise addition of phosgene solution (20% in toluene, 5.1 equiv) under an inert atmosphere. The reaction mixture was allowed to warm and stirred at 20–25 °C for another 2–16 h (Note: for the synthesis of compounds **60** and **61**, the reaction was stirred at −40 °C for 10 min.). The progress of the reaction was monitored by TLC using 20% EtOAc in PE as the mobile phase. Solvents were concentrated under vacuum and the residue obtained was dissolved in EtOAc. It was washed with H_2O and brine. The organic layer was dried over sodium sulfate, filtered and concentrated under vacuum to afford crude 1,3,4-oxadiazol-2-one which were purified by flash column chromatography using PE/EtOAc (9:1) as an eluent. The desired fractions were collected and solvents were evaporated on a rotatory evaporator to afford pure 1,3,4-oxadiazol-2-ones.

5.1.2. General procedures for preparation of novel 3-benzyl-1,3,4-oxadiazol-2(3*H*)-ones (51–53, 70 and 72)

To a solution of an appropriate nitro containing 3-benzyl-1,3,4-oxadiazol-2-one (**48**–**50**, **69** and **71**) (1.0 equiv) in methanol (0.28 M), 10% Pd/C (catalyst loading 10% w/w) was added and the mixture was stirred under an H_2 atmosphere at 20–25 °C for 4–8 h. The progress of the reaction was monitored by TLC using 40% EtOAc in PE as the mobile phase. Subsequently, the reaction mixture was filtered through Celite. The solvents were concentrated under vacuum and the residue obtained was dissolved in EtOAc and washed with H_2O and brine. The organic layer was dried over sodium sulfate, filtered and concentrated under vacuum to obtain a crude amino analogue which was purified by flash column chromatography using PE/EtOAc (8:2) as an eluent. The desired fractions were collected and solvents were evaporated on a rotatory evaporator to produce the pure desired amino containing 3-benzyl-1,3,4-oxadiazol-2-ones (**51**–**53**, **70** and **72**).

5.1.3. General procedures for preparation of novel 3-benzyl-1,3,4-oxadiazol-2(3*H*)-ones (54–59)

To a solution of an appropriate amino containing 3-benzyl-1,3,4-oxadiazol-2-one (**51**–**53**) (1.0 equiv) in dichloromethane (0.23 M), triethylamine (Et_3N) (2 equiv) was added followed by either acetyl chloride or benzoyl chloride (1 equiv) at 0–5 °C. The reaction mixture was allowed to warm to 22–25 °C and stirred at the same temperature for 16–24 h. The progress of the reaction was monitored by TLC using 20% EtOAc in PE as the mobile phase. Solvents were concentrated under vacuum and the residue obtained was dissolved in EtOAc and washed with H_2O and brine. The organic layer was dried over sodium sulfate, filtered and concentrated under vacuum to afford crude 3-benzyl-1,3,4-oxadiazol-2-one which were purified by flash column chromatography using PE/EtOAc (9:1) as an eluent. The desired fractions were collected and solvents were evaporated on a rotatory evaporator to afford pure acetamides (**54**–**56**) and benzamides (**57**–**59**).

5.1.4. 3-([1,1′-Biphenyl]-2-ylmethyl)-5-methoxy-1,3,4-oxadiazol-2(3*H*)-one (42)

Light orange oil (290 mg, 20%); ^{1}H NMR ($CDCl_3$): δ 7.44–7.41 (m, 2H), 7.37–7.34 (m, 6H), 7.28–7.25 (m, 1H), 4.78 (s, 2H), 3.92 (s, 3H); ^{13}C NMR ($CDCl_3$): δ 155.2, 151.5, 141.8, 140.2, 132.3, 130.4, 129.2, 128.4 (2C), 128.3, 128.0, 127.8, 127.6, 127.4, 57.6, 47.1; Anal. Calcd for $C_{16}H_{14}N_2O_3$: C, 68.08; H, 5.00; N, 9.92; Found: C, 68.12; H, 4.98; N, 9.89; ESI-MS: 283.03 $[M+H]^+$.

5.1.5. 5-Methoxy-3-(naphthalen-1-ylmethyl)-1,3,4-oxadiazol-2-(3*H*)-one (46)

White solid (100 mg, 13%); ^{1}H NMR ($CDCl_3$, 500 MHz): δ 8.19 (d, J = 8.5 Hz, 1H), 7.89–7.85 (m, 2H), 7.58 (t, J = 7.5 Hz, 1H), 7.52 (t, J = 7.2 Hz, 2H), 7.46 (t, J = 7.7 Hz, 1H), 5.22 (s, 2H), 3.89 (s, 3H); ^{13}C NMR (CDCl3): δ 155.6, 151.2, 133.8, 131.2, 130.4, 129.3, 128.8, 128.0, 126.9, 126.0, 125.2, 123.4, 57.3, 47.4; Anal. Calcd for $C_{14}H_{12}N_2O_3$: C, 65.62; H, 4.72; N, 10.93; Found: C, 65.66; H, 4.71; N, 10.95; ESI-MS: 257.06 $[M+H]^+$.

5.1.6. 5-Methoxy-3-(naphthalen-2-ylmethyl)-1,3,4-oxadiazol-2-(3*H*)-one (47)

White solid (135 mg, 17%); ^{1}H NMR ($CDCl_3$, 500 MHz): δ 7.85–7.83 (m, 3H), 7.80 (s, 1H), 7.50–7.45 (m, 3H), 4.94 (s, 2H), 3.93 (s, 3H); ^{13}C NMR (CDCl3): δ 155.6, 151.5, 133.2, 133.1, 132.4, 128.7, 127.9, 127.7, 127.4, 126.4, 126.3, 125.8, 57.4, 49.7; Anal. Calcd for $C_{14}H_{12}N_2O_3$: C, 65.62; H, 4.72; N, 10.93; Found: C, 65.59; H, 4.75; N, 10.91; ESI-MS: 257.07 $[M+H]^+$.

5.1.7. 5-Methoxy-3-(2-nitrobenzyl)-1,3,4-oxadiazol-2(3*H*)-one (48)

White solid (500 mg, 32%); ^{1}H NMR ($CDCl_3$, 500 MHz): δ 8.11 (d, J = 8.0 Hz, 1H), 7.65 (t, J = 7.25 Hz, 1H), 7.51 (t, J = 7.75 Hz, 1H), 7.39 (d, J = 8.0 Hz, 1H), 5.27 (s, 2H), 3.97 (s, 3H); ^{13}C NMR (CDCl3): δ 155.97, 151.53, 148.06, 133.89, 130.62, 129.26, 129.02, 125.35, 57.55, 46.67; Anal. Calcd for $C_{10}H_9N_3O_5$: C, 47.81; H, 3.61; N, 16.73; Found: C, 47.83; H, 3.58; N, 16.71; ESI-MS: 252.08 $[M+H]^+$.

5.1.8. 5-Methoxy-3-(4-nitrobenzyl)-1,3,4-oxadiazol-2(3*H*)-one (50)

White solid (387 mg, 91%); ^{1}H NMR ($CDCl_3$, 500 MHz): δ 8.24 (d, J = 8.5 Hz, 2H), 7.52 (d, J = 8.5 Hz, 2H), 4.88 (s, 2H), 3.97 (s, 3H); ^{13}C NMR (CDCl3): δ 155.9, 151.3, 147.9, 141.9, 129.0 (2C), 124.0 (2C), 57.5, 48.6; Anal. Calcd for $C_{10}H_9N_3O_5$: C, 47.81; H, 3.61; N, 16.73; Found: C, 47.80; H, 3.63; N, 16.75; ESI-MS: 252.05 $[M+H]^+$.

5.1.9. 3-(2-Aminobenzyl)-5-methoxy-1,3,4-oxadiazol-2(3*H*)-one (51)

Light yellow oil (295 mg, 89%); ^{1}H NMR ($CDCl_3$, 500 MHz): δ 7.22 (d, J = 7.5 Hz, 1H), 7.15 (t, J = 8.2 Hz, 1H), 6.74 (t, J = 7.2 Hz,

1H), 6.70 (d, *J* = 8.0 Hz, 1H), 4.70 (s, 2H), 4.24–4.22 (br s, 2H), 3.95 (s, 3H); ^{13}C NMR ($CDCl_3$): δ 155.6, 151.6, 145.6, 131.7, 130.1, 119.2, 118.3, 116.3, 57.4, 46.7; Anal. Calcd for $C_{10}H_{11}N_3O_3$: C, 54.30; H, 5.01; N, 19.00; Found: C, 54.28; H, 5.03; N, 19.02; ESI-MS: 222.20 $[M+H]^+$.

5.1.10. 3-(3-Aminobenzyl)-5-methoxy-1,3,4-oxadiazol-2(3*H*)-one (52)

Light yellow oil (385 mg, 50%); ^{1}H NMR ($CDCl_3$, 500 MHz): δ 7.18 (t, *J* = 7.75 Hz, 1H), 6.76 (d, *J* = 7.5 Hz, 1H), 6.68 (s, 1H), 6.66 (d, *J* = 8.0 Hz, 1H), 4.70 (s, 2H), 3.98 (s, 3H), 3.75–3.72 (br s, 2H); ^{13}C NMR (CDCl3): δ 155.5, 151.5, 146.8, 136.2, 129.7, 118.3, 114.9, 114.6, 57.3, 49.4; Anal. Calcd for $C_{10}H_{11}N_3O_3$: C, 54.30; H, 5.01; N, 19.00; Found: C, 54.31; H, 4.97; N, 18.97; ESI-MS: 222.11 $[M+H]^+$.

5.1.11. 3-(4-Aminobenzyl)-5-methoxy-1,3,4-oxadiazol-2(3*H*)-one (53)

Light cream-coloured solid (440 mg, 53%); ^{1}H NMR ($CDCl_3$, 500 MHz): δ 7.15 (d, *J* = 8.0 Hz, 2H), 6.65 (d, *J* = 8.0 Hz, 2H), 4.65 (s, 2H), 3.93 (s, 3H), 3.72–3.69 (br s, 2H); ^{13}C NMR ($CDCl_3$): δ 155.4, 151.3, 146.5, 129.7 (2C), 124.8, 115.1 (2C), 57.2, 49.1; Anal. Calcd for $C_{10}H_{11}N_3O_3$: C, 54.30; H, 5.01; N, 19.00; Found: C, 54.34; H, 4.98; N, 19.03; ESI-MS: 222.02 $[M+H]^+$.

5.1.12. *N*-(2-((5-Methoxy-2-oxo-1,3,4-oxadiazol-3(2*H*)-yl)-methyl)phenyl)acetamide (54)

White solid (105 mg, 71%); ^{1}H NMR ($CDCl_3$, 500 MHz): δ 8.67–8.65 (br s, 1H), 7.97 (d, *J* = 6.5 Hz, 1H), 7.39–7.37 (br s, 2H), 7.14 (s, 1H), 4.76 (s, 2H), 3.98 (s, 3H), 2.29 (s, 3H); ^{13}C NMR (CDCl3): δ 169.0, 155.7, 151.8, 136.6, 131.2, 129.9, 125.4, 125.0, 124.4, 57.6, 46.5, 24.3; Anal. Calcd for $C_{12}H_{13}N_3O_4$: C, 54.75; H, 4.98; N, 15.96; Found: C, 54.77; H, 4.97; N, 15.99; ESI-MS: 264.09 $[M+H]^+$.

5.1.13. *N*-(3-((5-Methoxy-2-oxo-1,3,4-oxadiazol-3(2*H*)-yl)-methyl)phenyl)acetamide (55)

Colourless oil (372 mg, 70%); ^{1}H NMR ($CDCl_3$, 500 MHz): δ 7.55 (d, *J* = 7.5 Hz, 1H), 7.44 (s, 1H), 7.31 (t, *J* = 7.7 Hz, 1H), 7.08 (d, *J* = 7.5 Hz, 1H), 4.75 (s, 2H), 3.95 (s, 3H), 2.17 (s, 3H), one –NH group; ^{13}C NMR ($CDCl_3$): δ 168.3, 155.6, 151.5, 138.4, 136.0, 129.5, 124.0, 119.7, 119.3, 57.4, 49.3, 24.6; Anal. Calcd for $C_{12}H_{13}N_3O_4$: C, 54.75; H, 4.98; N, 15.96; Found: C, 54.72; H, 5.02; N, 15.95; ESI-MS: 264.08 $[M+H]^+$.

5.1.14. *N*-(4-((5-Methoxy-2-oxo-1,3,4-oxadiazol-3(2*H*)-yl)-methyl)phenyl)acetamide (56)

Off-white solid (75 mg, 50%); ^{1}H NMR ($CDCl_3$, 500 MHz): δ 7.49 (d, *J* = 7.5 Hz, 2H), 7.30 (d, *J* = 7.5 Hz, 2H), 4.73 (s, 2H), 3.94 (s, 3H), 2.17 (s, 3H), one –NH gr.; ^{13}C NMR ($CDCl_3$): δ 168.3, 155.5, 151.4, 138.0, 130.8, 129.1 (2C), 120.0 (2C), 57.4, 49.0, 24.6; Anal. Calcd for $C_{12}H_{13}N_3O_4$: C, 54.75; H, 4.98; N, 15.96; Found: C, 54.74; H, 4.96; N, 15.94; ESI-MS: 264.05 $[M+H]^+$.

5.1.15. *N*-(2-((5-Methoxy-2-oxo-1,3,4-oxadiazol-3(2*H*)-yl)-methyl)phenyl)benzamide (57)

White solid (139 mg, 76%); ^{1}H NMR ($CDCl_3$, 500 MHz): δ 9.36–9.34 (br s, 1H), 8.0–7.90 (m, 3H), 7.47–7.14 (br s, 6H), 4.75 (s, 2H), 3.87 (s, 3H); ^{13}C NMR ($CDCl_3$): δ 166.1, 155.7, 151.3, 136.5, 134.4, 132.0, 131.2, 129.8, 128.6 (2C), 127.5 (2C), 126.8, 125.9, 125.7, 57.6, 46.3; Anal. Calcd for $C_{17}H_{15}N_3O_4$: C, 62.76; H, 4.65; N, 12.92; Found: C, 62.74; H, 4.63; N, 12.95; ESI-MS: 326.13 $[M+H]^+$.

5.1.16. *N*-(3-((5-Methoxy-2-oxo-1,3,4-oxadiazol-3(2*H*)-yl)-methyl)phenyl)benzamide (58)

Light yellow oil (156 mg, 82%); ^{1}H NMR ($CDCl_3$, 500 MHz): δ 7.89–7.86 (m, 3H), 7.70 (d, *J* = 8.0 Hz, 1H), 7.59–7.54 (m, 2H), 7.49 (t, *J* = 7.2 Hz, 2H), 7.37 (t, *J* = 7.7 Hz, 1H), 7.13 (d, *J* = 7.5 Hz, 1H), 4.78 (s, 2H), 3.95 (s, 3H); ^{13}C NMR (CDCl3): δ 165.7, 155.6, 151.5, 138.4, 136.0, 134.8, 131.9, 129.6, 129.3, 128.8, 128.5, 127.0, 124.2, 120.1, 119.7, 57.4, 49.3; Anal. Calcd for $C_{17}H_{15}N_3O_4$: C, 62.76; H, 4.65; N, 12.92; Found: C, 62.77; H, 4.68; N, 12.89; ESI-MS: 326.13 $[M+H]^+$.

5.1.17. *N*-(4-((5-Methoxy-2-oxo-1,3,4-oxadiazol-3(2*H*)-yl)-methyl)phenyl)benzamide (59)

White solid (125 mg, 68%); ^{1}H NMR (DMSO, 500 MHz): δ 10.30–10.27 (br s, 1H), 7.95 (d, *J* = 7.5 Hz, 2H), 7.76 (d, *J* = 8.0 Hz, 2H), 7.59 (d, *J* = 6.5 Hz, 1H), 7.53 (t, *J* = 7.2 Hz, 2H), 7.31 (d, *J* = 8.0 Hz, 2H), 4.76 (s, 2H), 3.93 (s, 3H); ^{13}C NMR (DMSO): δ 165.5, 155.0, 150.9, 138.8, 134.8, 131.6, 130.6, 128.3 (2C), 128.0 (2C), 127.6 (2C), 120.5 (2C), 57.7, 48.2; Anal. Calcd for $C_{17}H_{15}N_3O_4$: C, 62.76; H, 4.65; N, 12.92; Found: C, 62.79; H, 4.65; N, 12.94; ESI-MS: 326.07 $[M+H]^+$.

5.1.18. 3-(3-(Benzyloxy)benzyl)-5-methoxy-1,3,4-oxadiazol-2-(3*H*)-one (60)

Dark brown oil (396 mg, 56%) ^{1}H NMR ($CDCl_3$): δ 7.43–7.41 (m, 2H), 7.39–7.35 (m, 2H), 7.33–7.30 (m, 1H), 7.28–7.24 (m, 1H), 6.95–6.92 (m, 3H), 5.05 (s, 2H), 4.74 (s, 2H), 3.93 (s, 3H), ^{13}C NMR ($CDCl_3$): δ 159.1, 155.6, 151.4, 136.8, 136.5, 129.9, 128.6 (2C), 128.0, 127.5 (2C), 120.7, 114.7 (2C), 70.0, 57.4, 49.3; Anal. Calcd for $C_{17}H_{16}N_2O_4$: C, 65.38; H, 5.16; N, 8.97; Found: C, 65.41; H, 5.19; N, 9.01; ESI-MS: 313.14 $[M+H]^+$.

5.1.19. 3-(4-(Benzyloxy)benzyl)-5-methoxy-1,3,4-oxadiazol-2-(3*H*)-one (61)

Colourless oil (1.36 g, 55%); ^{1}H NMR ($CDCl_3$): δ 7.49–7.45 (m, 2H), 7.44–7.41 (m, 2H), 7.39–7.37 (m, 1H), 7.36–7.34 (m, 1H), 7.33–7.31 (m, 1H), 7.02–6.99 (m, 2H), 5.11 (s, 2H), 4.76 (s, 2H), 3.99 (s, 3H); ^{13}C NMR ($CDCl_3$): δ 158.8, 155.5, 151.3, 136.8, 129.8 (2C), 128.6 (2C), 128.0 (2C), 127.5 (2C), 115.1 (2C), 70.1, 57.3, 49.0; Anal. Calcd for $C_{17}H_{16}N_2O_4$: C, 65.38; H, 5.16; N, 8.97; Found: C, 65.39; H, 5.14; N, 8.99; ESI-MS: 312.89 $[M+H]^+$.

5.1.20. 3-((5-Methoxy-2-oxo-1,3,4-oxadiazol-3(2*H*)-yl)methyl)-benzonitrile (62)

White solid (137 mg, 18%); ^{1}H NMR ($CDCl_3$): δ 7.65–7.59 (m, 3H), 7.51–7.48 (m, 1H), 4.81 (s, 2H), 3.98 (s, 3H); ^{13}C NMR ($CDCl_3$): δ 155.8, 151.3, 136.5, 132.7, 132.1, 131.8, 129.8, 118.3, 113.1, 57.4, 48.6; Anal. Calcd for $C_{11}H_9N_3O_3$: C, 57.14; H, 3.92; N, 18.17; Found: C, 57.17; H, 3.88; N, 18.14; ESI-MS: 232.02 $[M+H]^+$.

5.1.21. 4-((5-Methoxy-2-oxo-1,3,4-oxadiazol-3(2*H*)-yl)methyl)-benzonitrile (63)

White solid (104 mg, 62% mg); ^{1}H NMR ($CDCl_3$): δ 7.68–7.62 (m, 2H), 7.47–7.45 (m, 2H), 4.84 (s, 2H), 3.97 (s, 3H); ^{13}C NMR ($CDCl_3$): δ 155.8, 151.3, 140.1, 132.7, 132.6, 128.9 (2C), 118.4, 112.4, 57.5, 48.9; Anal. Calcd for $C_{11}H_9N_3O_3$: C, 57.14; H, 3.92; N, 18.17; Found: C, 57.13; H, 3.90; N, 18.21; ESI-MS: 232.03 $[M+H]^+$.

5.1.22. Methyl 3-((5-methoxy-2-oxo-1,3,4-oxadiazol-3(2*H*)-yl)-methyl)benzoate (64)

White solid (1.8 g, 52%); ^{1}H NMR ($CDCl_3$): δ 8.07–8.01 (m, 2H), 7.55 (d, *J* = 7.6 Hz, 1H), 7.45 (t, *J* = 7.7 Hz, 1H), 4.83 (s, 2H), 3.95 (s, 3H), 3.92 (s, 3H); ^{13}C NMR ($CDCl_3$): δ 166.6, 155.7, 151.4, 135.4, 132.7, 130.8, 129.5, 129.3, 129.0, 57.4, 52.2, 49.0; Anal. Calcd for $C_{12}H_{12}N_2O_5$: C, 54.55; H, 4.58; N, 10.60; Found: C, 54.58; H, 4.61; N, 10.57; ESI-MS: 265.01 $[M+H]^+$.

5.1.23. Methyl 4-((5-methoxy-2-oxo-1,3,4-oxadiazol-3(2*H*)-yl)-methyl)benzoate (65)

White solid (687 mg, 52%); ^{1}H NMR ($CDCl_3$): δ 8.03 (d, *J* = 8.2 Hz, 2H), 7.41 (d, *J* = 8.1 Hz, 2H), 4.83 (s, 2H), 3.95 (s, 3H), 3.91 (s, 3H);

^{13}C NMR ($CDCl_3$): δ 166.6, 155.7, 151.4, 139.8, 130.1, 130.1 (2C), 128.1 (2C), 57.4, 52.2, 49.1; Anal. Calcd for $C_{12}H_{12}N_2O_5$: C, 54.55; H, 4.58; N, 10.60; Found: C, 54.56; H, 4.59; N, 10.64; ESI-MS: 265.0 $[M+H]^+$.

5.1.24. 5-Methoxy-3-(3-(trifluoromethyl)benzyl)-1,3,4-oxadiazol-2(3*H*)-one (66)

Colourless oil (455 mg, 55%); ^{1}H NMR ($CDCl_3$): δ 7.61–7.50 (m, 4H), 4.84 (s, 2H), 3.97 (s, 3H), ^{13}C NMR ($CDCl_3$): δ 155.8, 151.4, 135.9, 131.7, 131.2 (q, J_{CF} = 31.8 Hz), 129.5, 125.3, 125.2, 123.9 (q, J_{CF} = 272 Hz), 57.5, 48.9; Anal. Calcd for $C_{11}H_9F_3N_2O_3$: C, 48.18; H, 3.31; N, 10.22; Found: C, 48.21; H, 3.35; N, 10.25; ESI-MS: 293.11 $[M+NH_4]^+$.

5.1.25. 3-(3-Chlorobenzyl)-5-methoxy-1,3,4-oxadiazol-2(3*H*)-one (67)

Yellow oil (271 mg, 10%); ^{1}H NMR ($CDCl_3$): δ 7.36–7.32 (m, 1H), 7.31–7.28 (m, 2H), 7.24–7.22 (m, 1H), 4.75 (s, 2H), 3.96 (s, 3H); ^{13}C NMR ($CDCl_3$): δ 155.7, 151.4, 136.9, 134.7, 130.1, 128.5, 128.3, 126.4, 57.5, 48.8; Anal. Calcd for $C_{10}H_9ClN_2O_3$: C, 49.91; H, 3.77; N, 11.64; Found: C, 49.88; H, 3.75; N, 11.68; ESI-MS: 240.97 $[M+H]^+$.

5.1.26. 5-Methoxy-3-(3-methoxybenzyl)-1,3,4-oxadiazol-2(3*H*)-one (68)

Colourless oil (104 mg, 12%); ^{1}H NMR ($CDCl_3$): δ 7.29–7.25 (m, 1H), 6.92 (d, J = 7.6 Hz, 1H), 6.88–6.85 (m, 2H), 4.75 (s, 2H), 3.95 (s, 3H), 3.81 (s, 3H); ^{13}C NMR ($CDCl_3$): δ 159.9, 155.6, 151.4, 136.5, 129.9 (2C), 120.4, 113.7, 57.4, 55.3, 49.4; Anal. Calcd for $C_{11}H_{12}N_2O_4$: C, 55.93; H, 5.12; N, 11.86; Found: C, 55.96; H, 5.09; N, 11.82; ESI-MS: 237.05 $[M+H]^+$.

5.1.27. 5-Ethoxy-3-(3-nitrobenzyl)-1,3,4-oxadiazol-2(3*H*)-one (69)

Light cream-coloured solid (965 mg, 40%); ^{1}H NMR ($CDCl_3$): δ 8.22–8.19 (m, 2H), 7.70 (d, J = 7.2 Hz, 1H), 7.57 (t, J = 7.7 Hz, 1H), 4.88 (s, 2H), 4.34–4.30 (q, J = 6.7 Hz, 2H), 1.41 (t, J = 6.6 Hz, 3H); ^{13}C NMR ($CDCl_3$): δ 155.2, 151.3, 148.5, 131.0, 134.2, 129.9, 123.3, 123.1, 67.6, 48.5, 14.0; Anal. Calcd for $C_{11}H_{11}N_3O_5$: C, 49.81; H, 4.18; N, 15.84; Found: C, 49.84; H, 4.21; N, 15.87; ESI-MS: 266.0 $[M+H]^+$.

5.1.28. 3-(3-Aminobenzyl)-5-ethoxy-1,3,4-oxadiazol-2(3*H*)-one (70)

Light yellow oil (200 mg, 27%); ^{1}H NMR ($CDCl_3$): δ 7.13 (t, J = 7.7 Hz, 1H), 6.72 (d, J = 7.5 Hz, 1H), 6.65–6.62 (m, 2H), 4.66 (s, 2H), 4.32–4.28 (q, J = 7.1 Hz, 2H), 3.71–3.67 (br s, 2H), 1.39 (t, J = 6.6 Hz, 3H); ^{13}C NMR ($CDCl_3$): δ 154.8, 151.5, 146.8, 136.3, 129.7, 118.3, 114.9, 114.6, 67.2, 49.4, 14.1; Anal. Calcd for $C_{11}H_{13}N_3O_3$: C, 56.16; H, 5.57; N, 17.86; Found: C, 56.19; H, 5.53; N, 17.88; ESI-MS: 236.0 $[M+H]^+$.

5.1.29. 3-(3-Nitrobenzyl)-5-phenoxy-1,3,4-oxadiazol-2(3*H*)-one (71)

Light yellow solid (725 mg, 34%); ^{1}H NMR ($CDCl_3$): δ 8.21–8.19 (m, 2H), 7.68 (d, J = 7.5 Hz, 1H), 7.55 (t, J = 7.7 Hz, 1H), 7.43–7.40 (m, 2H), 7.30–7.26 (m, 3H), 4.90 (s, 2H); ^{13}C NMR ($CDCl_3$): δ 154.0, 151.6, 151.0, 148.5, 136.7, 134.2, 130.0 (2C), 129.7, 126.8, 123.5, 120.8 (2C), 119.4, 48.7; Anal. Calcd for $C_{15}H_{11}N_3O_5$: C, 57.51; H, 3.54; N, 13.41; Found: C, 57.53; H, 3.51; N, 13.37; ESI-MS: 314.06 $[M+H]^+$.

5.1.30. 3-(3-Aminobenzyl)-5-phenoxy-1,3,4-oxadiazol-2(3*H*)-one (72)

Light yellow oil (118 mg, 13%); ^{1}H NMR ($CDCl_3$): δ 7.39 (t, J = 7.8 Hz, 2H), 7.29–7.24 (m, 3H), 7.11 (t, J = 7.7 Hz, 1H), 6.71 (d, J = 7.3 Hz, 1H), 6.63 (t, J = 7.9 Hz, 2H), 4.69 (s, 2H), 3.71–3.69 (br s, 2H); ^{13}C NMR ($CDCl_3$): δ 153.4, 151.9, 151.1, 146.9, 136.0, 129.9 (2C), 129.8, 126.5 (2C), 118.3 (2C), 115.0, 114.6, 49.6; Anal. Calcd for $C_{15}H_{13}N_3O_3$: C, 63.60; H, 4.63; N, 14.83; Found: C, 63.58; H, 4.67; N, 14.79; ESI-MS: 284.11 $[M+H]^+$.

5.2. Biological evaluation

5.2.1. Determination of FAAH activity using anandamide as a substrate

The inhibitory activities of the synthesized compounds were determined using membranes of hFAAH-overexpressing COS-7 cells and [^{3}H]-AEA as the substrate, essentially as previously described.[42] Briefly, the assay buffer consisted of 50 mM Tris–HCl (pH 7.4) and 1 mM EDTA. The solvent for the test compounds was DMSO (the final concentration was 5% v/v max.). The incubations were performed in the presence of 0.5% (w/v) BSA (essentially fatty acid free). The inhibitors (5 μL) or DMSO were preincubated with hFAAH-COS-7 cell membranes (55 μL, 1 μg protein) for 10 min at 37 °C (60 μL). After 10 min, 20 μM AEA was added (final concentration 2 μM containing 10 nM of [^{3}H]-AEA; specific activity 60 Ci/mmol and 1 mCi/mL concentration). The final incubation volume was 100 μL. The incubations were carried out for 10 min at 37 °C. Ethyl acetate (400 μL) was added at the 20 min time point to stop the enzymatic reaction. Additionally, 100 μl of 50 mM Tris–HCl, pH 7.4; 1 mM EDTA was added. Then, samples were centrifuged for 4 min at RT 13,000 rpm, and aliquots (100 μL) from the aqueous phase containing [ethanolamine 1-^{3}H] were measured for radioactivity by liquid scintillation counting (Wallac 1450 MicroBeta; Wallac Oy, Finland).

5.2.2. Determination of MAGL activity using 2-AG as a substrate

The inhibitory activity of the synthesized compounds was determined using lysates of hMAGL overexpressing HEK293 cells and 2-AG as the substrate, essentially as previously described.[43] Briefly, the assay buffer consisted of 50 mM Tris–HCl (pH 7.4) and 1 mM EDTA. The solvent for the test compounds was DMSO (the final concentration was max 5% v/v). The incubations were performed in the presence of 0.5% (w/v) BSA (essentially fatty acid free). The inhibitors (5 μL) or DMSO were preincubated with lysates of hMAGL overexpressing HEK293 cells (2.5 μg) for 10 min at 37 °C (60 μL). At the 10 min time point, 2-AG (125 μM) was added to achieve the final concentration of 50 μM with the final incubation volume of 100 μL. Incubation was continued for 10 min at 37 °C. To stop the enzymatic reaction, 400 μL of cold 11 mM H_3PO_4 in ACN (the pH of the samples was simultaneously decreased to 3.0) was added to stabilize 2-AG against acyl migration to 1(3)-AG. All samples were centrifuged for 4 min at RT 14,000 rpm. The formation of arachidonic acid and depletion of 2-AG (and 1(3)-AG) were measured by HPLC.[43]

5.2.3. Determination of ABHD6 and ABHD12 activities

Glycerol production from the 1-AG hydrolysis was determined with a sensitive fluorescent glycerol assay using lysates of HEK293 cells transiently overexpressing hABHD6 or hABHD12 as previously described.[16,34] In this assay, glycerol production is coupled via a three-step enzymatic cascade to hydrogen peroxide-dependent generation of resorufin whose fluorescence (λ_{ex} 530; λ_{em} 590 nm) is kinetically monitored using a Tecan Infinite M200 plate reader (Tecan Group Ltd, Männedorf, Switzerland). Briefly, hABHD6- or hABHD12-HEK293 lysates (99 μL, 0.3 μg protein/well) were pretreated for 30 min with the solvent (DMSO) or the inhibitor with desired concentrations (1 μL), after which 1-AG (100 μL, 12.5 μM final concentration) was added. The reaction was then kinetically monitored for 90 min. The assays contain routinely 0.5% (w/v) BSA (essentially fatty acid free) as a carrier. 1-AG was

used instead of 2-AG, as this is the preferred endocannabinoid isomer for hABHD6 and hABHD12.[16] The IC_{50}-values at the 90 min time-point were calculated after nonlinear fitting of the inhibitors' dose–response curves. Assay blanks without hABHD6 (or hABHD12) lysates were included in each experiment and fluorescence of the assay blank was subtracted before calculation of the final results. The reversibility of compounds to inhibit hABHD6 was tested in a 96-well plate format using the 40-fold-dilution method previously described for testing reversibility of MAGL inhibitors.[34]

5.2.4. Activity-based protein profiling (ABPP) of serine hydrolases

Competitive ABPP using mouse whole brain membranes was conducted to visualize the selectivity of inhibitors towards ABHD6 against serine hydrolases in brain membrane proteome. We used the active site serine-targeting fluorescent fluorophosphonate probe TAMRA-FP as previously described.[16,34] Briefly, brain membranes (100 μg) were treated for 1 h with DMSO or the selected inhibitors, after which TAMRA-FP labelling was conducted for 1 h at RT (final probe concentration 2 μM). The reaction was quenched by addition of 2× gel loading buffer, after which 10 μg protein per lane was added into the gel and the proteins were resolved in 10% SDS–PAGE together with molecular weight standards. Finally, TAMRA-FP labelling was visualized (λ_{ex} 552; λ_{em} 575 nm) using a fluorescent scanner (FLA-3000 laser fluorescence scanner, Fujifilm, Tokyo, Japan).

5.2.5. Data analyses

Data analyses for the concentration–response curves were calculated from non-linear regressions using Graph Pad Prism 5.0 for Windows. For comparison of potency values in reversibility assays, statistical analysis was performed by using one-way Anova, followed by Tukey's multiple comparison test.

5.3. Molecular modelling

Molecular modelling was performed using the Schrödinger Maestro software package.[44] The homology model of ABHD6 was constructed as previously reported.[21] In our homology modelling studies, we assumed that the catalytic triad of ABHD6 comprised Ser148-His306-Asp278 and the oxyanion hole was formed by Met149 and Phe80. The structure of the small molecule was prepared using the LigPrep module of Schrodinger suite. Prior to the Glide docking studies, the grid box was centred closest to the active site residues in the case of ABHD6 model (Phe80, Ser148, Met149, Ile203, His306). The ligand docking was performed using default SP settings of the Schrodinger Glide using hydrogen bond constraints to oxyanion hole residues (at least one contact required). Graphical illustrations were generated using MOE software (Molecular Operating Environment (MOE), 2014.09).[45]

In the reversibility studies, compounds were optimized with B3LYP DFT and 6-31++G(d,p) basis set of Gaussian09.[46] Gaussian09 was also used to calculate frontier molecular orbitals. Transition states complexes of compounds JZP-169 (**52**), JZP-430 (**7**), KT182 (**5**), WWL70 (**1**) and THL were built with Ser^{148} which was attached to the carbonyl group of these compounds. QM/MM energy minimization was performed with the appropriate module of Discovery Studio 3.1[47] and CHARMM force field for two sets of the system: for transition state complexes and for ligands in covalent complexes with the enzyme, after reaction with Ser^{148}. The implementation of QM/MM in Discovery Studio 3.1 involves DMol3 (DFT) for the QM region, CHARMM force field for the MM region and QUANTUMM, a communication program between the two regions. Ligands and binding site residues as recognized by Discovery Studio 3.1 were treated as the quantum region. The calculated energies were used to calculate energy of dissociation of covalent complexes.

Acknowledgments

We thank Ms. Tiina Koivunen, Ms. Minna Glad, Ms. Taija Hukkanen, Ms. Satu Marttila and Ms. Miriam Lopez Navarro for their skillful technical assistance. CSC—Scientific Computing, Ltd is gratefully acknowledged for software licenses and computational resources. The Centre of International Mobility (CIMO, Grant TM-09-6221 for J.Z.P.), Graduate School of Drug Design, UEF (for J.Z.P.), The Academy of Finland (Grants 139140 for T.J.N., 127653 for T.P., 139620 for J.T.L.) and Biocenter Finland/DDCB have provided financial support for this study. Part of the research was performed under the Marie Curie IEF fellowship for A.A.K. The calculations with Gaussian09 were performed under a computational Grant from the Interdisciplinary Center for Mathematical and Computational Modeling (ICM), Warsaw, Poland, Grant number G30-18. Dr. Ewen Macdonald and Dr. Gerald G. Netto are acknowledged for revising the language of this manuscript. J.Z.P. has provided a personal fund for language editing.

Supplementary data

Supplementary data (synthesis and spectroscopic characterization of all intermediates (**22**–**37**); inhibitory activities of novel oxadiazolones **42**, **46**–**72** towards ABHD12; selectivity of compound **72** among the serine hydrolases of the mouse brain membrane proteome using competitive ABPP; inhibitory activity of selected compounds **52** and **72** towards ABHD6 and related references, NMR-spectra of selected compounds **52** and **72**) associated with this article can be found, in the online version, at http://dx.doi.org/10.1016/j.bmc.2015.08.030.

References and notes

1. Blankman, J. L.; Simon, G. M.; Cravatt, B. F. *Chem. Biol.* **2007**, *14*, 1347.
2. Mechoulam, R.; Ben-Shabat, S.; Hanus, L.; Ligumsky, M.; Kaminski, N. E.; Schatz, A. R.; Gopher, A.; Almog, S.; Martin, B. R.; Compton, D. R.; Pertwee, R. G.; Griffin, G.; Bayewitch, M.; Barg, J.; Vogel, Z. *Biochem. Pharmacol.* **1995**, *50*, 83.
3. Sugiura, T.; Kondo, S.; Sukagawa, A.; Nakane, S.; Shinoda, A.; Itoh, K.; Yamashita, A.; Waku, K. *Biochem. Biophys. Res. Commun.* **1995**, *215*, 89.
4. Savinainen, J. R.; Saario, S. M.; Laitinen, J. T. *Acta Physiol.* **2012**, *204*, 267.
5. Tchantchou, F.; Zhang, Y. *J. Neurotrauma* **2013**, *30*, 565.
6. Alhouayek, M.; Masquelier, J.; Cani, P. D.; Lambert, D. M.; Muccioli, G. G. *Proc. Natl. Acad. Sci. U.S.A.* **2013**, *110*, 17558.
7. Thomas, G.; Betters, J. L.; Lord, C. C.; Brown, A. L.; Marshall, S.; Ferguson, D.; Sawyer, J.; Davis, M. A.; Melchior, J. T.; Blume, L. C.; Howlett, A. C.; Ivanova, P. T.; Milne, S. B.; Myers, D. S.; Mrak, I.; Leber, V.; Heier, C.; Taschler, U.; Blankman, J. L.; Cravatt, B. F.; Lee, R. G.; Crooke, R. M.; Graham, M. J.; Zimmermann, R.; Brown, H. A.; Brown, J. M. *Cell Rep.* **2013**, *5*, 508.
8. Naydenov, A.; Horne, E.; Cheah, C.; Swinney, K.; Hsu, K.; Cao, J.; Marrs, W.; Blankman, J.; Tu, S.; Cherry, A.; Fung, S.; Wen, A.; Li, W.; Saporito, M.; Selley, D.; Cravatt, B.; Oakley, J.; Stella, N. *Neuron* **2014**, *83*, 361.
9. Lichtman, A. H.; Blankman, J. L.; Cravatt, B. F. *Mol. Pharmacol.* **2010**, *78*, 993.
10. Chanda, P. K.; Gao, Y.; Mark, L.; Btesh, J.; Strassle, B. W.; Lu, P.; Piesla, M. J.; Zhang, M.; Bingham, B.; Uveges, A.; Kowal, D.; Garbe, D.; Kouranova, E. V.; Ring, R. H.; Bates, B.; Pangalos, M. N.; Kennedy, J. D.; Whiteside, G. T.; Samad, T. A. *Mol. Pharmacol.* **2010**, *78*, 996.
11. Schlosburg, J. E.; Blankman, J. L.; Long, J. Z.; Nomura, D. K.; Pan, B.; Kinsey, S. G.; Nguyen, P. T.; Ramesh, D.; Booker, L.; Burston, J. J.; Thomas, E. A.; Selley, D. E.; Sim-Selley, L.; Liu, Q.; Lichtman, A. H.; Cravatt, B. F. *Nat. Neurosci.* **2010**, *13*, 1113.
12. Fiskerstrand, T.; H'mida-Ben Brahim, D.; Johansson, S.; M'zahem, A.; Haukanes, B. I.; Drouot, N.; Zimmermann, J.; Cole, A. J.; Vedeler, C.; Bredrup, C.; Assoum, M.; Tazir, M.; Klockgether, T.; Hamri, A.; Steen, V. M.; Boman, H.; Bindoff, L. A.; Koenig, M.; Knappskog, P. M. *Am. J. Hum. Genet.* **2010**, *87*, 410.
13. Marrs, W. R.; Blankman, J. L.; Horne, E. A.; Thomazeau, A.; Lin, Y. H.; Coy, J.; Bodor, A. L.; Muccioli, G. G.; Hu, S. S.; Woodruff, G.; Fung, S.; Lafourcade, M.; Alexander, J. P.; Long, J. Z.; Li, W.; Xu, C.; Moeller, T.; Mackie, K.; Manzoni, O. J.; Cravatt, B. F.; Stella, N. *Nat. Neurosci.* **2010**, *13*, 951.
14. Li, W.; Blankman, J. L.; Cravatt, B. F. *J. Am. Chem. Soc.* **2007**, *129*, 9594.
15. Marrs, W. R.; Horne, E. A.; Ortega-Gutierrez, S.; Cisneros, J. A.; Xu, C.; Lin, Y. H.; Muccioli, G. G.; Lopez-Rodriguez, M.; Stella, N. *J. Biol. Chem.* **2011**, *286*, 28723.
16. Navia-Paldanius, D.; Savinainen, J. R.; Laitinen, J. T. *J. Lipid Res.* **2012**, *53*, 2413.

17. Bachovchin, D. A.; Ji, T.; Li, W.; Simon, G. M.; Blankman, J. L.; Adibekian, A.; Hoover, H.; Niessen, S.; Cravatt, B. F. *Proc. Natl. Acad. Sci. U.S.A.* **2010**, *107*, 20941.
18. Hsu, K.; Tsuboi, K.; Adibekian, A.; Pugh, H.; Masuda, K.; Cravatt, B. F. *Nat. Chem. Biol.* **2012**, *8*, 999.
19. Hsu, K.; Tsuboi, K.; Chang, J. W.; Whitby, L. R.; Speers, A. E.; Pugh, H.; Cravatt, B. F. *J. Med. Chem.* **2013**, *56*, 8270.
20. Janssen, F. J.; Deng, H.; Baggelaar, M. P.; Allarà, M.; van, d. W.; den Dulk, H.; Ligresti, A.; van Esbroeck, Annelot C. M.; McGuire, R.; Di Marzo, V.; Overkleeft, H. S.; van, d. S. *J. Med. Chem.* **2014**, *57*, 6610.
21. Patel, J. Z.; Nevalainen, T. J.; Savinainen, J. R.; Adams, Y.; Laitinen, T.; Runyon, R. S.; Vaara, M.; Ahenkorah, S.; Kaczor, A. A.; Navia-Paldanius, D.; Gynther, M.; Aaltonen, N.; Joharapurkar, A. A.; Jain, M. R.; Haka, A. S.; Maxfield, F. R.; Laitinen, J. T.; Parkkari, T. *ChemMedChem* **2015**, *10*, 253.
22. Ben Ali, Y.; Chahinian, H.; Petry, S.; Muller, G.; Lebrun, R.; Verger, R.; Carrière, F.; Mandrich, L.; Rossi, M.; Manco, G.; Sarda, L.; Abousalham, A. *Biochemistry* **2006**, *45*, 14183.
23. Muccioli, G. G.; Labar, G.; Lambert, D. M. *ChemBioChem* **2008**, *9*, 2704.
24. Minkkilä, A.; Savinainen, J. R.; Käsnänen, H.; Xhaard, H.; Nevalainen, T.; Laitinen, J. T.; Poso, A.; Leppänen, J.; Saario, S. M. *ChemMedChem* **2009**, *4*, 1253.
25. Point, V.; Pavan Kumar, K. V. P.; Marc, S.; Delorme, V.; Parsiegla, G.; Amara, S.; Carriere, F.; Buono, G.; Fotiadu, F.; Canaan, S.; Leclaire, J.; Cavalier, J. *Eur. J. Med. Chem.* **2012**, *58*, 452.
26. Delorme, V.; Diomandé, S. V.; Dedieu, L.; Cavalier, J.; Carrière, F.; Kremer, L.; Leclaire, J.; Fotiadu, F.; Canaan, S. *PLoS One* **2012**, *7*, e46493.
27. Kiss, L. E.; Ferreira, H. S.; Beliaev, A.; Torrão, L.; Bonifáciob, M. J.; Learmonth, D. A. *Med. Chem. Commun.* **2011**, *2*, 889.
28. Käsnänen, H.; Minkkilä, A.; Taupila, S.; Patel, J. Z.; Parkkari, T.; Lahtela-Kakkonen, M.; Saario, S. M.; Nevalainen, T.; Poso, A. *Eur. J. Pharm. Sci.* **2013**, *49*, 423.
29. Patel, J. Z.; Parkkari, T.; Laitinen, T.; Kaczor, A. A.; Saario, S. M.; Savinainen, J. R.; Navia-Paldanius, D.; Cipriano, M.; Leppänen, J.; Koshevoy, I. O.; Poso, A.; Fowler, C. J.; Laitinen, J. T.; Nevalainen, T. *J. Med. Chem.* **2013**, *56*, 8484.
30. Savinainen, J. R.; Patel, J. Z.; Parkkari, T.; Navia-Paldanius, D.; Marjamaa, J. J. T.; Laitinen, T.; Nevalainen, T.; Laitinen, J. T. *PLoS One* **2014**, *9*, e109869/1.
31. Patel, J. Z.; Ahenkorah, S.; Vaara, M.; Staszewski, M.; Adams, Y.; Laitinen, T.; Navia-Paldanius, D.; Parkkari, T.; Savinainen, J. R.; Walczyński, K.; Laitinen, J. T.; Nevalainen, T. J. *Bioorg. Med. Chem. Lett.* **2015**, *25*, 1436.
32. Savinainen, J. R.; Saario, S. M.; Niemi, R.; Järvinen, T.; Laitinen, J. T. *Br. J. Pharmacol.* **2003**, *140*, 1451.
33. Savinainen, J. R.; Kokkola, T.; Salo, O. M. H.; Poso, A.; Järvinen, T.; Laitinen, J. T. *Br. J. Pharmacol.* **2005**, *145*, 636.
34. Aaltonen, N.; Savinainen, J. R.; Ribas, C. R.; Rönkkö, J.; Kuusisto, A.; Korhonen, J.; Navia-Paldanius, D.; Häyrinen, J.; Takabe, P.; Käsnänen, H.; Pantsar, T.; Laitinen, T.; Lehtonen, M.; Pasonen-Seppänen, S.; Poso, A.; Nevalainen, T.; Laitinen, J. T. *Chem. Biol.* **2013**, *20*, 379.
35. Borgstrom, B. *Biochim. Biophys. Acta* **1988**, *962*, 308.
36. Hadvary, P.; Sidler, W.; Meister, W.; Vetter, W.; Wolfer, H. *J. Biol. Chem.* **1991**, *266*, 2021.
37. Parkkari, T.; Haavikko, R.; Laitinen, T.; Navia-Paldanius, D.; Rytilahti, R.; Vaara, M.; Lehtonen, M.; Alakurtti, S.; Yli-Kauhaluoma, J.; Nevalainen, T.; Savinainen, J. R.; Laitinen, J. T. *PLoS One* **2014**, *9*, e98286/1.
38. Savinainen, J. R.; Yoshino, M.; Minkkilä, A.; Nevalainen, T.; Laitinen, J. T. *Anal. Biochem.* **2010**, *399*, 132.
39. Lodola, A.; Rivara, S.; Mor, M. *Adv. Protein Chem. Struct. Biol.* **2011**, *85*, 1.
40. Bowman, A. L.; Makriyannis, A. *Chem. Biol. Drug Des.* **2013**, *81*, 382.
41. Scudder, P. H. *Electron Flow in Organic Chemistry: A Decision-Based Guide to Organic Mechanisms*, 2nd ed.; Wiley, 2013.
42. Saario, S. M.; Poso, A.; Juvonen, R. O.; Järvinen, T.; Salo-Ahen, O. M. H. *J. Med. Chem.* **2006**, *49*, 4650.
43. Minkkilä, A.; Saario, S. M.; Käsnänen, H.; Leppänen, J.; Poso, A.; Nevalainen, T. *J. Med. Chem.* **2008**, *51*, 7057.
44. *Schrödinger Release 2014-4: Maestro, version 10.0; Ligprep, version 3.2; Protein Preparation Wizard: Epik version 3.0, impact version 6.5, prime version 3.8.; Glide, version 6.5*; Schrödinger, LLC: New York, NY, 2014.
45. *Molecular Operating Environment (MOE), 2014.09*; Chemical Computing Group Inc.: 1010 Sherbooke St. West, Suite #910, Montreal, QC, Canada, H3A 2R7, 2014.
46. Frisch, M. J.; Trucks, G. W.; Schlegel, H. B.; Scuseria, G. E.; Robb, M. A.; Cheeseman, J. R.; Montgomery, J. A.; Vreven, T.; Kudin, K. N.; Burant, J. C.; Millam, J. M.; Iyengar, S. S.; Tomasi, J.; Barone, V.; Mennucci, B.; Cossi, M.; Scalmani, G.; Rega, N.; Petersson, G. A.; Nakatsuji, H.; Hada, M.; Ehara, M.; Toyota, K.; Fukuda, R.; Hasegawa, J.; Ishida, M.; Nakajima, T.; Honda, Y.; Kitao, O.; Nakai, H.; Klene, M.; Li, X.; Knox, J. E.; Hratchian, H. P.; Cross, J. B.; Bakken, V.; Adamo, C.; Jaramillo, J.; Gomperts, R.; Stratmann, R. E.; Yazyev, O.; Austin, A. J.; Cammi, R.; Pomelli, C.; Ochterski, J. W.; Ayala, P. Y.; Morokuma, K.; Voth, G. A.; Salvador, P.; Dannenberg, J. J.; Zakrzewski, V. G.; Dapprich, S.; Daniels, A. D.; Strain, M. C.; Farkas, O.; Malick, D. K.; Rabuck, A. D.; Raghavachari, K.; Foresman, J. B.; Ortiz, J. V.; Cui, Q.; Baboul, A. G.; Clifford, S.; Cioslowski, J.; Stefanov, B. B.; Liu, G.; Liashenko, A.; Piskorz, P.; Komaromi, I.; Martin, R. L.; Fox, D. J.; Keith, T.; Al-Laham, M. A.; Peng, C. Y.; Nanayakkara, A.; Challacombe, M.; Gill, P. M. W.; Johnson, B.; Chen, W.; Wong, M. W.; Gonzalez, C.; Pople, J. A. *Gaussian 09*; Gaussian: Wallingford CT, 2009.
47. Discovery Studio, v. 3.1, Accelrys.